

STUDIES OF NEARBY POOR CLUSTERS: THE ERIDANUS GROUP

C. N. A. WILLMER, P. FOCARDI,^{a)} L. NICOLACI DA COSTA, AND P. S. PELLEGRINI

Departamento de Astronomia, CNPq/Observatório Nacional, Rua General José Cristino 77, 20921 São Cristovão, Rio de Janeiro, Brazil

Received 1 May 1989; revised 5 June 1989

ABSTRACT

We have made a dynamical study of the Eridanus group of galaxies. This system is quite prominent in one of the large-scale features found in the recently completed Southern Sky Redshift Survey: the Eridanus–Fornax–Dorado filament. The irregular aspect of Eridanus suggests the existence of subclustering, which is confirmed by statistical tests. These subclusters are bound, suggesting that the system is still condensing from the Hubble flow and may eventually form a cluster of about $10^{14} M_{\odot}$. By calculating the two-body orbital solution, we find that the Eridanus complex and the Fornax Cluster also form a bound system, though still in the expansion phase.

I. INTRODUCTION

The great increase of information available from extensive redshift surveys has motivated a renewed interest on studies of the structure and dynamical properties of groups and clusters of galaxies. One of the major outcomes of the larger amount of data has been the detection of substructures in clusters, confirming earlier results based on two-dimensional data (e.g., Geller and Beers 1982; Baier 1983). However, there is still some controversy on how frequently subclustering occurs in clusters, since its detection could be affected by Poisson noise, or due to chance superpositions of nearby unbound groups (e.g., Cancer, Bothun *et al.* 1983). As a matter of fact, the use of different statistical methods devised to identify substructures has given discordant results even when applied to the same data (West and Bothun 1988, hereafter referred to as WB; Dressler and Shectman 1988).

Subclustering could have different origins: it could be caused by clumps of galaxies that are still merging to form a cluster, or due to the infall of outlying groups into an already relaxed system (e.g., WB). As pointed out by West, Oemler, and Dekel (1988, hereafter referred to as WOD) the study of the properties of subclustering is important because it may provide information concerning the nature of the initial density fluctuation spectrum, which could, in principle, allow one to discriminate between different cosmogonic scenarios. Recent studies of clusters with a large number of available redshifts have suggested that subclustering is quite common (e.g., Dressler and Shectman 1988), and may be present in the cores of clusters that have a regular appearance such as Coma (Fitchett and Webster 1988) and Hydra (Fitchett and Merritt 1988), or even in clusters with dominant cD galaxies with velocities significantly displaced from the cluster mean (e.g., A1795, Hill *et al.* 1988; Oegerle, Fitchett, and Hoessel 1989; A2670, Sharples, Ellis, and Gray 1988). However, the detection of subclustering in the central regions of clusters has always been liable to large uncertainties as this has usually been done through galaxy counts, carried out in regions that present a high local background. For instance, WOD find that the presence of substructure in the inner regions of rich clusters is not very frequent, and in many cases could be due to Poisson noise. However, even when radial velocities are available, a clear separation of subclusters in the central regions of clusters can be difficult as this depends on the relative projection of clumps on the plane of

the sky. On the other hand, WB find that subclustering, which can be considered as significant, tends to occur preferentially in the outer parts of clusters and seems to be correlated with the surrounding supercluster structure in which these are embedded. These authors suggest that the subclustering in these cases should not be interpreted as evidence of nonrelaxation, and that rich clusters are in general relaxed systems. The observational evidence seems to be that rich clusters may have relaxed cores but are still growing by the continuous infall of bound groups.

To understand the processes at work during the formation of clusters and their subsequent evolution, it is important to study systems spanning a larger range of physical parameters (Geller 1988). However, in contrast to rich clusters, the study of poor clusters (e.g., Beers *et al.* 1984; Geller *et al.* 1984) has not been often carried out, as the determination of some of their physical parameters is subject to larger uncertainties than is the case for the richer systems. For instance, due to the smaller number of members and their irregular aspect, parameters such as core radii or radial-velocity dispersion profiles are not so easily obtained, or can even be meaningless. On the other hand, due to their irregular morphology, it is likely that these are not relaxed systems, and so may still contain some imprints of the processes that were important at earlier epochs and that have not been fully smeared out yet.

When examining the maps of the Southern Sky Redshift Survey (SSRS, da Costa *et al.* 1988) one finds that most of the nearby clusters sampled belong to this class of object, like the Fornax, Dorado, and Eridanus groups, which lie in a nearby “filamentary” structure, that apparently extends for about 15 Mpc ($H_0 = 100$ km/s/Mpc), at a distance of about 15 Mpc of the Local Group. In this paper we study the Eridanus group using the data available in the Southern Galactic Cap (SGC) sample, being prepared by Pellegrini *et al.* (1989). The main interest in this study is to determine the dynamical properties of such poor systems, as their loose and clumpy appearance would make them difficult to detect at larger distances, yet may represent an important phase of cluster formation.

The concentration of galaxies in Eridanus has been known for many years (e.g., Baker 1933, 1936), and the complexity of the region was further discussed by de Vaucouleurs (1975), who found that his group 31 together with galaxies associated to N1332 and N1209 formed what he termed the “Eridanus Cloud.” The dynamical parameters were first published by Rood, Rothman, and Turnrose (1970), using

^{a)} On leave from Dipartimento di Astronomia, Università di Bologna.

the de Vaucouleurs (1975) identification. Further studies followed, by Sandage and Tammann (1975) and Welch, Chincarini, and Rood (1975), who increased the number of available radial velocities in the region. In particular, the latter authors called attention to the possible dynamical connection between the Eridanus and Fornax clusters. More recently, with the availability of more extensive redshift data, the assignment of galaxies to the group has been made applying group-finding algorithms to an all-sky shallow sample by Huchra and Geller (1982), and by Maia, da Costa, and Latham (1989, hereafter referred to as MdCL), using the deeper SSRS sample.

As Eridanus lies near the northern cut of the ESO/Uppsala catalog (Lauberts 1982), this study will use a magnitude-limited sample of the SGC, so to avoid biases generated by the ESO/Uppsala cut. In Sec. II we define the galaxy sample and describe the distribution of galaxies in the region of interest, presenting some dynamical parameters for the cluster. Section III describes the results from the various substructure tests, a discussion on the dynamical state of the cluster follows in Sec. IV, and some conclusions are drawn in Sec. V.

II. THE DISTRIBUTION OF GALAXIES

The region containing the Eridanus cluster is shown in Fig. 1, where we have plotted galaxies selected from the SGC sample. This is a merge of the ESO/Uppsala (Lauberts 1982), the MCG (Vorontsov-Velyaminov and Arkhipova 1963-1968), and the Zwicky *et al.* (1961-1968) catalogs, limited at approximately $B(0) = 14.5$. The magnitudes for the MCG catalog were corrected by adding 0.5 mag to make them consistent with the Zwicky magnitudes, following Huchra (1976). For the Lauberts (1982) catalog, the magnitudes were estimated from mean relations between diame-

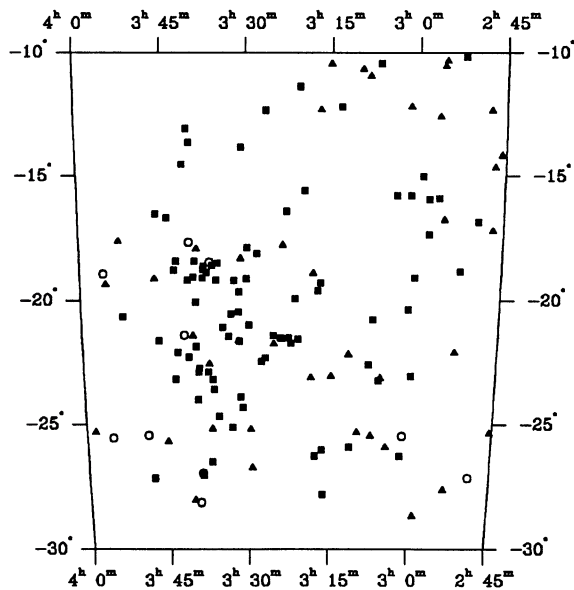


FIG. 1. Map of the Southern Galactic Cap sample, limited at 14.5 mag, containing galaxies in the general direction of Eridanus. Open circles represent galaxies without redshifts, while filled squares represent galaxies with radial velocities smaller than 3500 km/s and filled triangles objects with radial velocities larger than that value.

ters and magnitudes for galaxies which had these available. Further details can be found in Pellegrini (1988).

The extent shown in Fig. 1 was chosen examining the SGC maps so galaxies that might be associated with the Eridanus–Fornax–Dorado feature lying in the vicinity of Eridanus would be included, as this group’s boundaries are not well defined. The limits were estimated from those maps to be $2^{\text{h}} 45^{\text{m}}$ and 4^{h} in right ascension and -30° and -10° in declination. The same limits can be inferred inspecting the slightly deeper SSRS sample (da Costa *et al.* 1988). The southern limit corresponds to what is roughly “halfway” between Eridanus and Fornax, and where there is a dearth of galaxies with radial velocities less than 3000 km/s.

The total number of galaxies in this region is 139 and only ten do not have a measured radial velocity, making the sample 93% complete. Galaxies with no available redshift are shown in Fig. 1 as open circles, while filled squares and triangles denote galaxies that have radial velocities smaller and larger than 3500 km/s, respectively. All of the galaxies without redshifts, most of which are late spirals or dwarfs, have low surface brightness and are difficult objects to obtain optical spectra. However, these objects lie far from the group center, and their effect on the overall dynamics is probably small. Eridanus is fairly prominent in the eastern portion of the plot, at around $3^{\text{h}} 38^{\text{m}}$ and -21° . Some of the galaxies that lie towards the western part of the plot, were assigned to the MdCL groups 71 ($3^{\text{h}} 15^{\text{m}}$, -26°) and 78 ($3^{\text{h}} 07^{\text{m}}$, -22°), which have a dispersed appearance.

The histogram in redshift space for galaxies contained in Fig. 1, can be seen in Fig. 2, where we used bins of 200 km/s width, after correcting for galactic rotation of 300 km/s. The peak due to the Eridanus–Fornax–Dorado filament is very prominent, and contains over 50% of the galaxy sample. The next peak at about 4000 km/s is due to a smooth distribution of galaxies in the background of Eridanus, which is possibly connected to the wall described by da Costa *et al.* (1988). The galaxies at about 500 km/s and beyond 2800 km/s are not likely to belong to the Eridanus–Fornax–Dorado feature. This can be clearly seen in the wedge diagram in declination shown in Fig. 3, where we have used a slightly larger region in declination, because it allows a better definition of the cluster and the relationship with its surroundings. In this figure we can see at about -35° the outskirts of Fornax. The

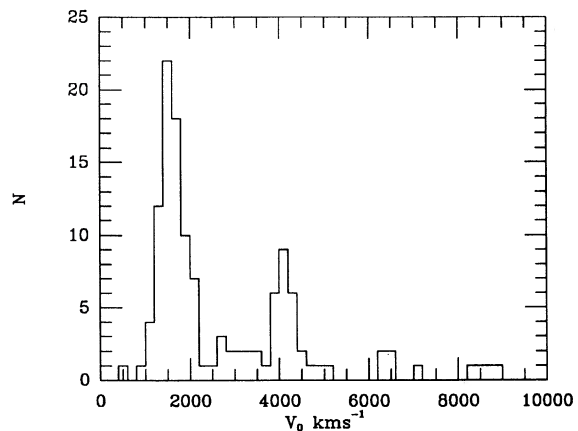


FIG. 2. Radial-velocity distribution of galaxies contained in Fig. 1.

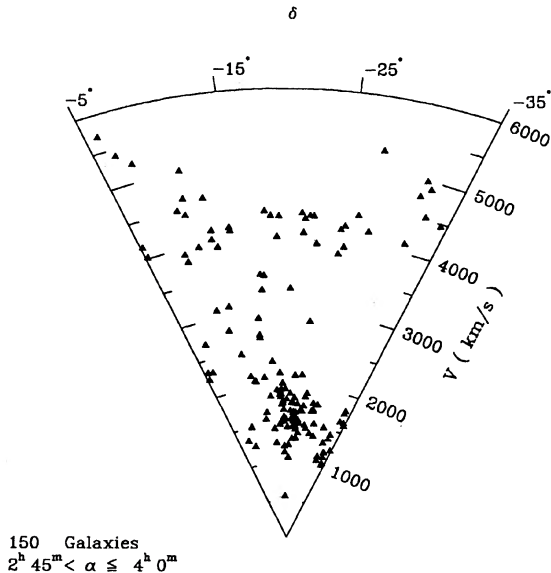


FIG. 3. Wedge diagram for galaxies in the declination range of -35° to -5° , in the same right ascension range as Fig. 1.

“wall” mentioned by da Costa *et al.* (1988) is fairly prominent in the background, at around 4500 km/s. Neither in this figure nor in Fig. 1 can one see any inhomogeneities caused by merging the different catalogs.

The examination of these figures suggests that the Eridanus group is concentrated between the approximate limits of $3^{\text{h}} 15^{\text{m}}$ and 4^{h} in right ascension and -26° and -15° in declination. These positional limits will be considered henceforth as constituting the cluster boundaries, while the cluster sample will be defined as those galaxies within these limits that have radial velocities differing by less than three standard deviations from the cluster mean velocity as determined below, and contains a total of 54 galaxies. The galaxies that lie in this direction having radial velocities smaller than 6000 km/s are presented in Table I, where the identification, position, and morphological classification were taken from the Lauberts (1982) or MCG catalogs. We also show the estimated magnitudes, heliocentric velocities, and associated errors. The reference column indicates whether the redshift was compiled in the ESO catalog (E and reference number therein), while the remaining redshifts were taken from Pellegrini *et al.* (1989). Finally, the capital letters in the last column indicate the subcluster assignment for some galaxies (see below and Sec. III), while an asterisk denotes objects considered as belonging either to the foreground or the background of the cluster.

A plot of galaxies that belong to the cluster sample is shown in Fig. 4, where we discriminate between early types (squares) and late types (triangles). It can be seen that the cluster has a very irregular and clumpy appearance, with no obvious center. An inspection of the figure suggests that Eridanus may contain three or four large subcondensations, one at about $3^{\text{h}} 40^{\text{m}}$, -19° (clump “A”), another at $3^{\text{h}} 40^{\text{m}}$, -23° (B), a slightly elongated feature at $3^{\text{h}} 20^{\text{m}}$, -21° (C), which is the group associated with N1332, that was first identified by de Vaucouleurs (1975), and finally a somewhat loose grouping of galaxies centered at $3^{\text{h}} 32^{\text{m}}$ and -21° (see also Fig. 8 below). There are four elliptical galaxies, 18 SO’s and 32 spirals; this makes a percentile population mix of 7%/33%/60%, which is similar to that of spiral-rich

clusters (Bahcall 1977).

Some physical parameters for Eridanus are presented in Table II, where we have made the assumption that the system is virialized. The agreement between MdCL and this work is quite good, in spite of the difference between the samples. There we give the coordinates of the geometrical center, the mean radial velocity, as well as some dynamical parameters. The errors for these parameters were estimated using the treatment of Danese, De Zotti, and di Tullio (1980) for the velocity dispersion (σ_v) and virial mass (M_{VT}), and the “statistical jackknife” (e.g., Bothun *et al.* 1983) for the other parameters. For all the parameters derived from the velocity dispersion, we have used σ_{v_c} , which has had the errors associated to redshift and uncertainties removed, following the precepts given in the reference above. The harmonic radius (R_{H}) and the mean pairwise separation (R_{p}) were calculated using the formulas in MdCL and Huchra and Geller (1982), respectively; the crossing time (T_c) was calculated using the latter authors’ formula. For the mass we have also used some of the estimators proposed by Heisler, Tremaine, and Bahcall (1985), namely the projected mass (M_{p}) and average mass (M_{av}), which present some advantages, such as numerical stability, with respect to the virial mass. All these mass estimators show a reasonable agreement when calculated for Eridanus, and are comparable to those of groups of similar richness (MdCL; Geller and Huchra 1983; Bothun *et al.* 1983; Hopp and Materne 1985). Of course, we should stress that the virialization assumption may not be completely valid, as shall be seen in Sec. III.

The radial-velocity distribution of the cluster sample is shown in Fig. 5, where we have used 100 km/s bins. The distribution is fairly regular, although there could be a slight skewness, with a larger number of galaxies towards the low-velocity end, and a secondary peak at about 1850 km/s. Some of the tests suggested by Yahil and Vidal (1977) that can quantify the departure from normality (i.e., from a Gaussian distribution), have been applied to the cluster sample, namely the $a, b_1^{1/2}, b_2$ (Pearson and Hartley 1970), and u tests (Pearson and Stephens 1964). The $b_1^{1/2}$ measures the skewness of the distribution, while the a, b_2 , and u are more sensitive to its kurtosis. The values we find for the statistics are $a = 0.8069$, $b_2 = 2.6375$, $b_1^{1/2} = 0.0872$, and $u = 4.2573$, none of them allowing the rejection of normality at a significance level $< 10\%$. A more detailed discussion of these tests can be found in the original references, as well as tables containing the confidence levels. We should note that the result from the u test may be questionable, as the sample has been cleared of a very discordant redshift. These results imply that if any substructure is present, it cannot be evidenced either through the velocity distribution, which has no significant departure from normality, nor through the cluster’s velocity dispersion, which would be much larger than observed if there were substructure along the line of sight.

III. DETERMINATION OF SUBSTRUCTURE

Even though the statistical tests on the velocity distribution do not detect significant departures from normality, and the dynamical parameters are comparable to those of groups of similar richness, the clumpiness of Eridanus suggests that substructure may exist and influence the dynamics of the cluster. In order to quantify the degree of substructure, we have applied a variety of tests that would allow us to estimate

TABLE I. Galaxies in the cluster region.

Identification	R.A.	Dec.	m_B	T	cz	+/-	R	C
NGC 1297	3 16 58	-19 16 54	13.0	0	1550	28		
NGC 1300	3 17 25	-19 35 30	11.5	6	1583	8	E9	
NGC 1301	3 18 19	-18 53 42	14.2	6	4023	27		*
MCG -3-9-28	3 19 48	-15 35 00	12.5	5	2138	10		
NGC 1315	3 20 53	-21 33 12	13.8	-2	1673	26		C
MCG -3-9-33	3 21 32	-19 55 48	13.9	6	1838	8	E93	
NGC 1325	3 22 12	-21 43 06	12.7	8	1596	15	E3	C
NGC 1325A	3 22 35	-21 30 48	13.8	4	1314	60		C
MCG -3-9-41	3 23 06	-16 25 00	14.5	5	1878	15		
NGC 1329	3 23 45	-17 45 54	14.5	1	4371	33		*
ESO 548 G16	3 23 49	-21 31 00	12.5	5	2161	39		C
NGC 1332	3 24 04	-21 30 36	11.6	-2	1477	19	E3	C
IC 1928	3 25 16	-21 44 00	14.5	1	4266	27		*
MCG -4-9-14	3 25 22	-21 24 06	14.1	6	1657	33		C
MCG -4-9-15	3 26 48	-22 18 42	14.0	1	1471	65		
NGC 1347	3 27 30	-22 27 00	14.2	6	1775	41		
MCG -3-9-48	3 28 19	-18 06 42	14.4	1	1502	34		
NGC 1353	3 29 49	-20 59 06	12.7	3	1577	24		
MCG -3-10-3	3 30 02	-17 53 12	13.8	8	1961	8	E93	
MCG -3-10-5	3 30 13	-19 06 54	14.3	0	1699	29		
MCG -4-9-24	3 30 52	-24 18 06	14.2	1	1926	37		
MCG -3-10-6	3 31 13	-18 18 48	14.2	6	4303	31		*
IC 1952	3 31 16	-23 52 48	13.9	4	1759	58		
IC 1953	3 31 29	-21 38 42	12.7	6	1860	8	E93	
NGC 1359	3 31 32	-19 39 30	13.0	6	1976	8	E93	
MCG -4-9-28	3 31 38	-21 37 18	14.0	8	4082	47		*
NGC 1362	3 31 39	-20 26 54	14.1	-2	1233	29		
MCG -3-10-11	3 32 28	-19 11 42	13.4	1	1606	26		
NGC 1371	3 32 52	-25 06 00	12.0	1	1462	7	E3	
NGC 1370	3 33 01	-20 32 18	13.8	-2	1063	28		
IC 1962	3 33 25	-21 27 24	13.7	7	1788	36		
NGC 1377	3 34 26	-21 03 54	13.8	-2	1792	30		
NGC 1385	3 35 19	-24 40 00	12.1	3	1502	13	E2	
NGC 1383	3 35 33	-18 30 06	14.0	-2	1948	19		A
NGC 1390	3 35 37	-19 10 18	13.9	-2	1215	33		
MCG -4-9-38	3 36 07	-23 34 54	14.2	-2	1687	37		B
NGC 1395	3 36 19	-23 11 24	11.6	-5	1702	21	E3	B
NGC 1393	3 36 23	-18 35 24	13.8	-2	2185	26		A
NGC 1403	3 37 00	-22 33 00	12.9	-5	4310	28		*
NGC 1401	3 37 11	-22 53 06	13.6	-2	1518	28		B
NGC 1400	3 37 16	-18 51 00	12.5	-3	549	21		*
IC 343	3 37 52	-18 36 18	14.3	-2	1869	30		A
NGC 1407	3 37 57	-18 44 30	11.2	-3	1766	21		A
MCG -3-10-31	3 38 04	-19 05 30	14.4	-2	1817	27		A
NGC 1415	3 38 46	-22 43 24	13.0	1	1564	9	E3	B
NGC 1416	3 38 52	-22 52 42	14.4	-2	2167	24		B

TABLE I. (continued)

Identification	R.A.			Dec.			m_B	T	cz	+/-	R	C
MCG -4-9-50	3	39	05	-23	59	48	13.9	3	1877	9		
MCG -3-10-34	3	39	18	-20	03	54	14.1	-2	1471	46		
NGC 1422	3	39	19	-21	50	30	14.0	4	1619	45		
IC 346	3	39	29	-18	25	36	13.6	1	1897	47		A
MCG -3-10-36	3	39	41	-19	03	12	14.2	1	2053	31		A
MCG -4-9-52	3	39	51	-21	24	12	14.4	0	4341	26		*
NGC 1426	3	40	38	-22	16	06	12.7	-5	1443	6	E3	
MCG -3-10-39	3	40	43	-19	10	48	14.3	3	1134	36		A
NGC 1439	3	42	39	-22	04	42	13.0	-5	1670	10	E3	
NGC 1440	3	42	48	-18	25	24	13.1	-2	1534	27	E3	
NGC 1438	3	43	07	-23	09	30	14.1	3	1524	36		
NGC 1452	3	43	07	-18	47	24	13.3	1	1904	17		
MCG -3-10-45	3	44	18	-16	41	00	14.5	5	1264	27		
NGC 1459	3	44	51	-25	40	36	13.9	6	4210	23		*
MCG -4-10-2	3	46	03	-21	37	36	13.5	3	1548	35		
MCG -3-10-47	3	46	12	-16	32	00	13.5	-2	1450	36		
MCG -3-10-4	3	46	37	-19	07	48	14.4	6	4295	29		*
NGC 1482	3	52	57	-20	38	54	13.8	1	1916	39		
MCG -4-10-1	3	58	20	-25	19	18	13.9	6	4154	15		*

Notes to TABLE I

E2, E3, E93 Reference in Lauberts (1982)
 Otherwise Pellegrini et al. (1989)

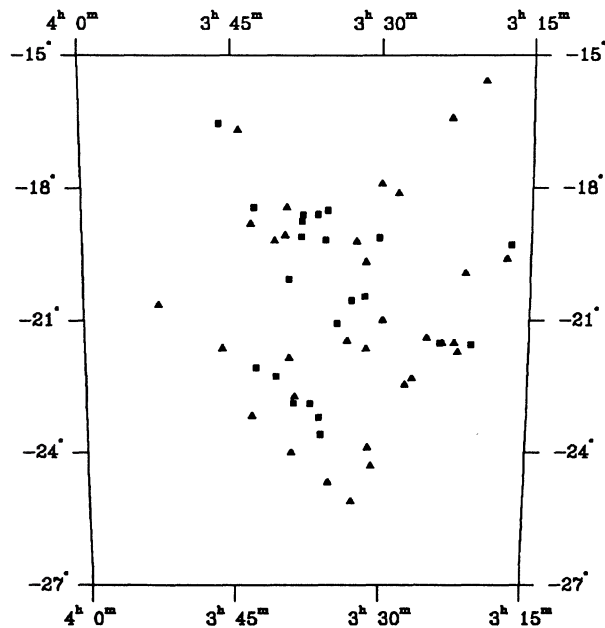


FIG. 4. Map of galaxies belonging to the cluster sample. Early types are represented by squares and late types by triangles.

TABLE II. Cluster parameters.

α		$3^h 33.6^m$
δ		$-20^\circ 37'$
N_g		54
V_0	(km/s)	1579 ± 5
σ_v	(km/s)	265
σ_{vc}	(km/s)	$261 (+30, -22)$
R_H	(Mpc)	1.97 ± 0.02
R_p	(Mpc)	1.29 ± 0.01
M_{VT}	($10^{13} M_\odot$)	$9.38 (+2.2, -1.7)$
M_p	($10^{13} M_\odot$)	11.30 ± 0.32
M_{av}	($10^{13} M_\odot$)	9.17 ± 0.19
T_c	(Hubbles)	0.20

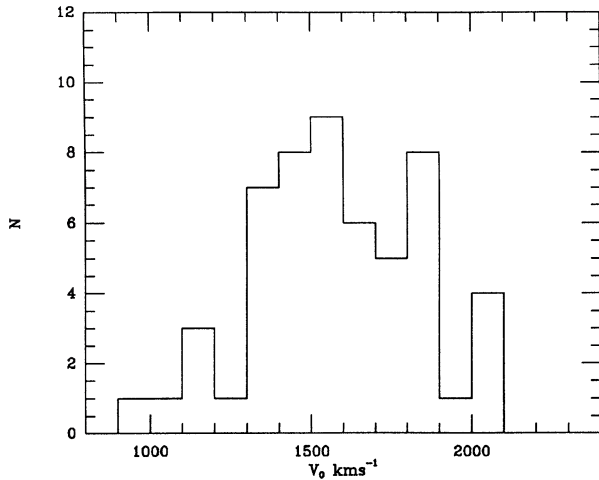


FIG. 5. Radial-velocity distribution for the cluster sample.

its significance and at the same time to assign galaxies to subclusters in an objective way.

One test designed to detect the existence of substructure is the two-dimensional Lee function, which has been proposed by Fitchett (1988) and used by Fitchett and Webster (1987) to analyze the central regions of Coma. This method compares statistics related to the two-dimensional distribution of galaxies, which are obtained by projecting each galaxy's coordinates onto a line and determining for each point the values of the mean and dispersion towards its left and right (σ_l and σ_r , respectively). The ratio, $L(\gamma) = \{[\sigma_l/(\sigma_l + \sigma_r)] - 1\}$ is found, where σ_l is the dispersion for the whole set. The line is then rotated (in our case, in a W to N sense) and for each angle γ , two parameters are determined, L_{\max} , which is the maximum value of $L(\gamma)$, and L_{rat} , which is the ratio between the maximum and minimum values of $L(\gamma)$. In both cases, the maximum value of the statistics occurs when the line connects the "centers" of the subclusters (Fit-

chett and Webster 1987). The significance of the results is estimated by means of Monte Carlo simulations, which consist in scrambling the galaxies "azimuthal" angles, while keeping the radial distance fixed, therefore maintaining the radial profile (Fitchett and Webster 1987). The results for these parameters calculated for Eridanus are shown in Fig. 6. The comparison with Monte Carlo simulations showed that L_{\max} in 21% of the simulations presented higher or comparable values to those obtained for the cluster, while for L_{rat} this happened in 34% of the cases. However, this weak level of significance can be due to the fact that the Lee function is more sensitive to binary structures (Fitchett 1988), which is not the case for Eridanus.

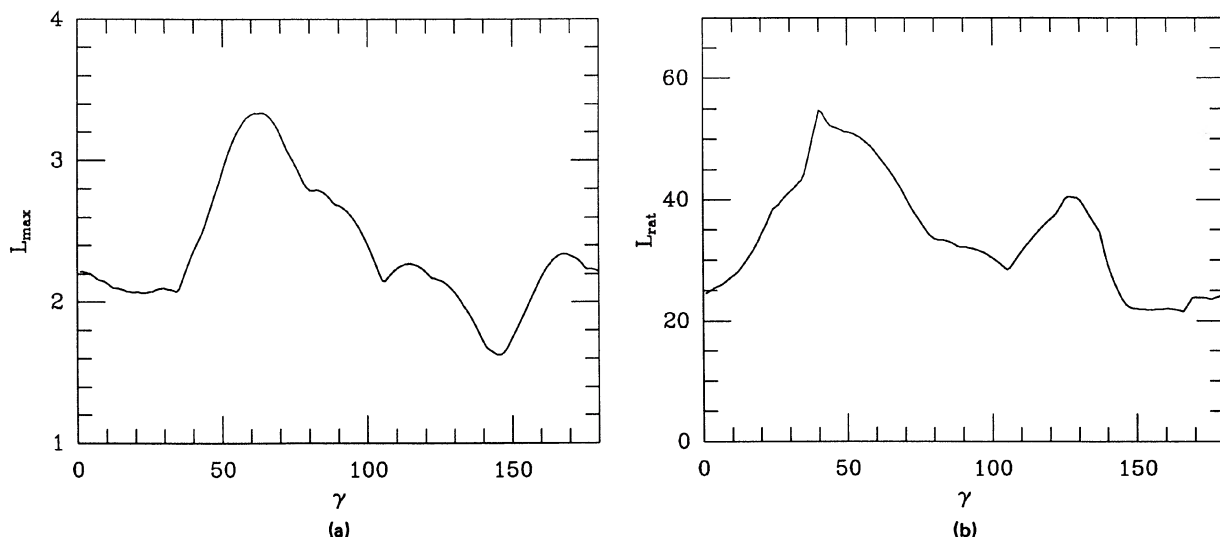
Three further tests sensitive to substructure were developed by WOD. These are the symmetry test (β), which is sensitive to the overall regularity or irregularity of the cluster, the angular separations (θ), which measures the spectrum of distances between pairs of galaxies, and finally, the density contrast test, which we will discuss further on. The first two tests are more adequate for cases when the substructure is in the form of a localized asymmetry superimposed on a symmetric and rather regular distribution. The β parameter is defined as

$$\beta = N^{-1} \sum \frac{d_{oi}}{d_i},$$

where d_i is the average distance between a galaxy and its five nearest neighbors, while d_{oi} is the mean distance of the five nearest galaxies to a symmetrical point in relation to the cluster center. We should note that the definition of β we use differs from that of WOD in the sense that they used the logarithm of the parameter we have adopted here. The angular separation parameter is defined as

$$\theta = \left\{ [2/N(N-1)] \sum_{i>j} \theta_{ij}^{-1} \right\}^{-1},$$

where θ_{ij} is the angular separation between galaxies i and j , the sum being calculated over all galaxy pairs. As a check on the noise that may affect these tests, we applied them to a few hundred model clusters with King profiles. We found that in

FIG. 6. Plot of the Lee function. (a) shows the L_{\max} estimator and (b) the L_{rat} estimator.

this ideal case the distribution has a peak at $\beta = 1$, as expected, and falls rapidly, so that only about 4% of the cases have β values higher than 1.5, the highest being 2.5. For θ , the distribution is much more symmetrical, peaking between 1.0 and 1.1, and lying between roughly 0.6 and 1.5.

In contrast to WOD, who use as the center the point of highest density, and due to the lack of an obvious center in Eridanus, we have used the geometrical center as origin for calculating β and θ . These were computed in four radial intervals, each containing 12 galaxies. The choice of 12 was a compromise between the available number of galaxies per ring and the number of rings themselves; the main conclusions still hold if a smaller number of rings that contain more galaxies are used. As the comparison of Eridanus with model clusters would always give evidence of substructure, we have used the simulations as described above, for the Lee function. Using this method, we detect the presence of subclustering in all but the innermost ring, but with different significance levels. In Fig. 7 we show the distribution of the β values obtained in these simulations and the value we find for

the cluster in each ring. The angular separation test gives essentially the same results, the second ring showing the strongest signal, which is not unexpected, as this is the ring where most of the subclusters lie. Table III shows the values of the outer radius in degrees from the geometric center, β , θ , and $\Delta\theta$ (the uncertainty associated to θ) for each ring.

The density contrast test, which is not affected by the shape of the distribution, consists in using a “friends-of-friends” technique to assign galaxies to individual clumps, using different density contrast levels. According to WOD the substructure can be considered as significant when, as one goes towards higher contrast levels, the cluster fragments into smaller “clumps” that contain at least 20% of the cluster’s total mass. When building the groups, we did not use radial-velocity information, but only the projected coordinates. This method has the disadvantage that contamination by interlopers cannot be controlled. On the other hand, the narrow velocity range and the small numbers we are dealing with make it meaningless to define a quasi-three-dimensional group finding parameter space. The mean sur-

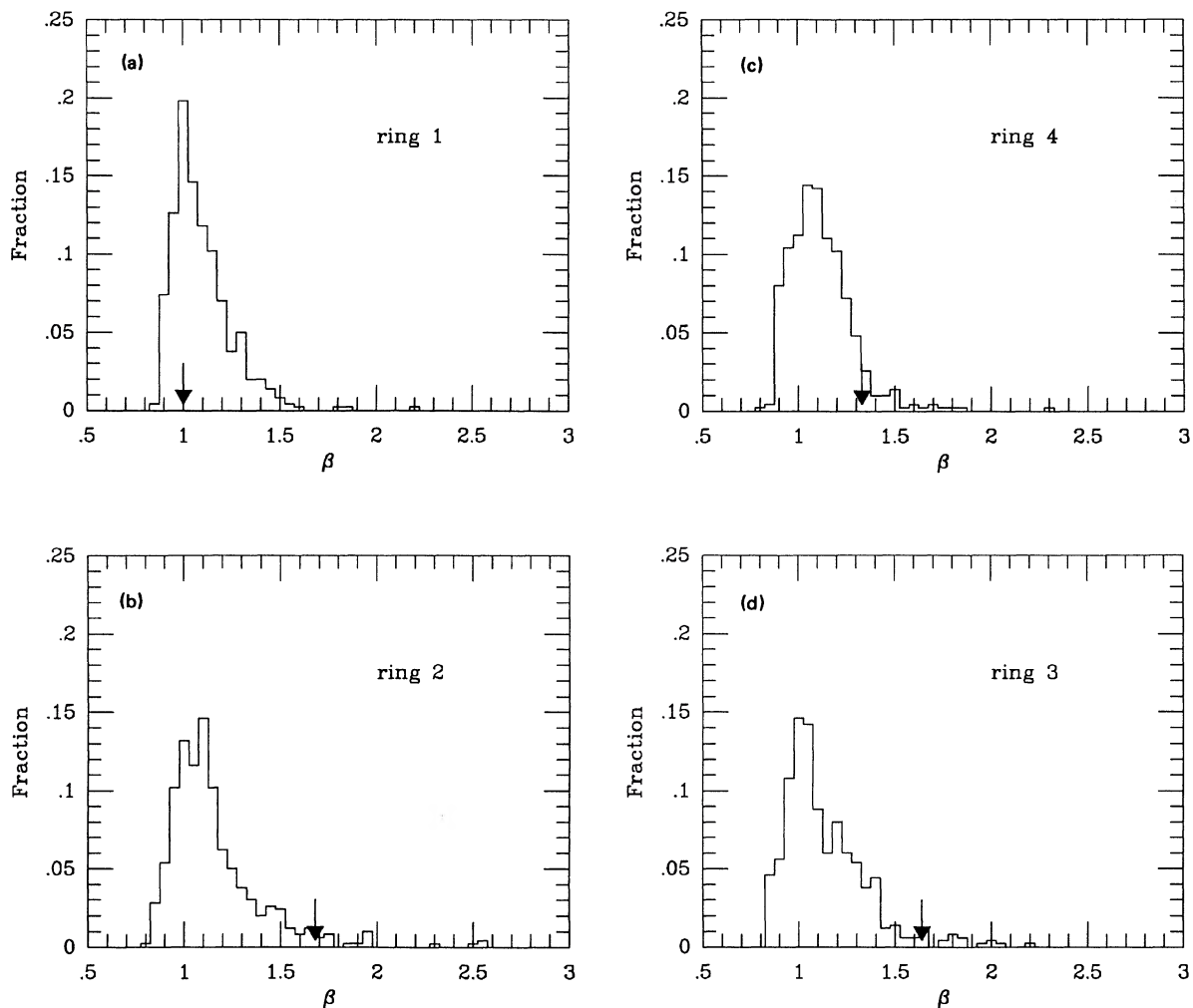


FIG. 7. Normalized distribution of β values, obtained from 500 simulations, and calculated for each ring. The arrow indicates the β value for the cluster (see Table III).

TABLE III. Subclustering estimators.

radius (degrees)	β	θ	$\Delta\theta$
1.83	1.00	1.21	0.27
2.41	1.68	0.73	0.18
2.90	1.64	0.88	0.19
4.27	1.33	1.02	0.25

face density was defined from the number of galaxies in the cluster sample and the solid angle it occupies. We found substructure that could be considered as significant only at a level of $\delta\rho/\rho = 2$, and the most important “subclusters” are to be found at the radial distance from the cluster center where the two previous tests gave the most significant results. The clumps are fairly stable down to the lowest contrast level, where the radius used to detect “friends-of-friends” was set equal to the average separation. Table I identifies those galaxies that were assigned to the three larger clumps using a density contrast of $\delta\rho/\rho = 1$. The galaxy assignment we obtain using this (surface) density contrast is quite similar to that found using the group-finding algorithm of Huchra and Geller (1982) at a (volumetric) density contrast of 1000 for the SSRS group catalog (Maia, private communication). The large difference in the density contrast level is due to the adopted operative definitions. MdCL use a “global” value for the mean density, defined from the entire galaxy sample, while we use a “local” value, calculated as the average density within the region of interest, which already has a significant density enhancement.

Roughly the same clumps are found using an approach similar to that of Geller and Beers (1982), making contours by counting galaxies in bins of 0.25 Mpc (corresponding to 52.5 arcmin at the cluster’s mean distance), with 50% overlap, and subtracting a uniform background corresponding to the mean density of the cluster. The isopleths are constructed in steps of one galaxy per bin, to the maximum of five in a bin, and the final result is shown in Fig. 8. This test was originally designed to be applied to data for which few redshifts were available, in order to extract from the bidimensional samples all the information possible. However, even though it has some shortcomings, we find that this test gives a good visual impression of the subcluster determination using the density contrast test of WOD.

Finally, we have applied the test developed by Dressler and Shectman (1988) to determine the presence of subclustering that combines positional and velocity data, and that is sensitive to substructure well separated on the sky and in velocity. The statistic they proposed compares local values of the mean radial velocity and dispersion to the mean cluster values, using the ten nearest objects for each galaxy. We also used other values for the number of neighbors (5 and 8) to calculate the local mean velocity and dispersion. In no case did we find significant evidence of subclustering. However, as noted by WB, some of the statistical tests that are sensitive to velocity separation (e.g., that devised by

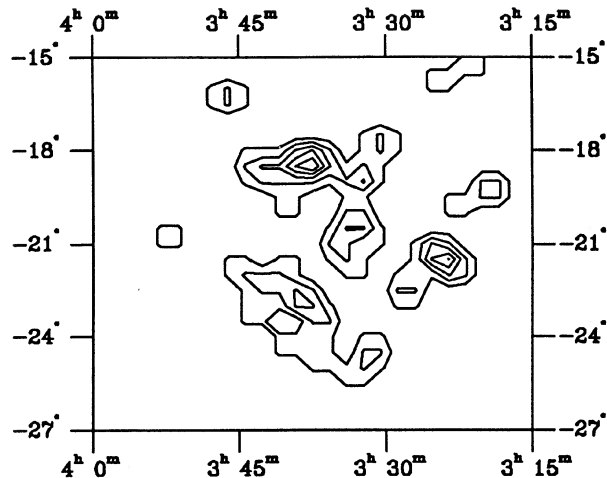


FIG. 8. Contour plot for the cluster sample.

Dressler and Shectman 1988) give stronger evidence of substructure in systems that present large velocity gaps between subcomponents, and that may have no physical connection.

The score for this cluster is that the three tests of WOD detect subclustering that could be considered as significant, while the Lee function and the Dressler and Shectman (1988) test give no strong evidence for its existence. However, the fact that the group-finding algorithm identifies the same clumps at a high-density contrast (Maia, private communication), does lend some support to our interpretation that these could possibly be “bona fide” physical systems.

IV. DYNAMICS

In order to analyze the dynamics of each subcluster, and the cluster as a whole, we have used the density contrast test (Sec. III) at $\delta\rho/\rho = 1$ to assign galaxies to individual groups. We only considered those groups containing at least five galaxies, so as to have relatively stable dynamical parameters. The distributions in radial velocity for the individual clumps, as well as for the unassigned galaxies are shown in Fig. 9. In contrast to the Cancer cluster (Bothun *et al.* 1983), here we can see that the shape of the distribution for the unassigned galaxies does not differ much from that of the whole sample (Fig. 5), and that there is no significant spread in radial velocity between the different clumps and unassigned galaxies. This is further confirmed when calculating some of the physical parameters for the subclusters, as in Sec. II, and that are presented in Table IV. This table shows that all subclusters lie at a similar radial velocity, the greatest difference being between clumps A and C, of about 200 km/s, less than the velocity dispersion of any of the subclusters. As these groups were constructed using a two-dimensional algorithm, some contamination may be expected. The inspection of Fig. 9 shows that the only subcluster which allows for some suspicion is clump A, where one galaxy has a radial velocity somewhat smaller than the clump mean, but, due to the small number of members, this may not be very significant. Furthermore, the mean parameters for the subclusters are rather stable as one goes to lower density contrast levels, and the comparison with results obtained by Maia (private communication) using different volumetric

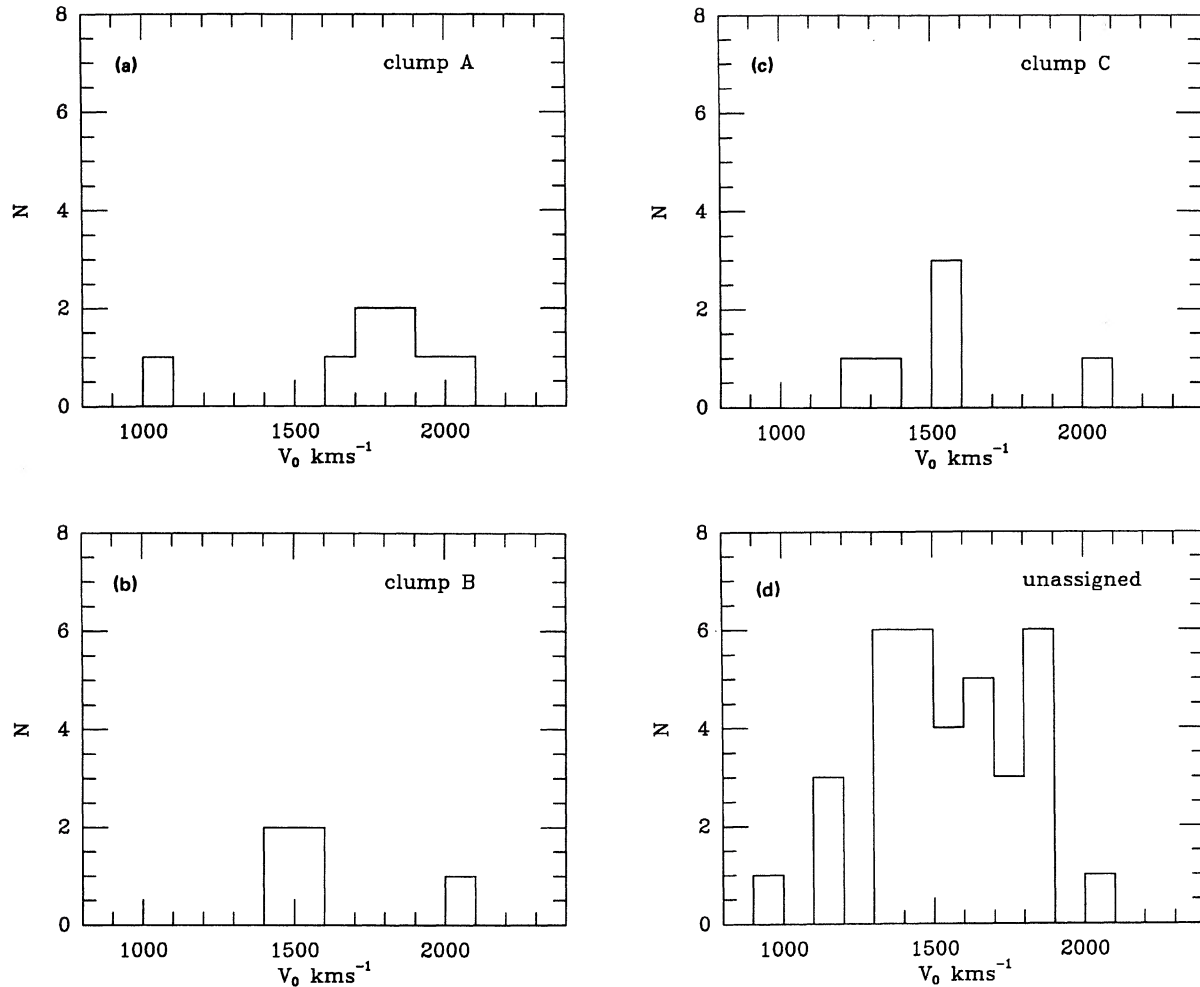


FIG. 9. Velocity distribution of galaxies assigned to subclusters and of unassigned galaxies.

density contrast levels for the SSRS sample, shows a rather good agreement.

Clump A has the most concentrated appearance (Fig. 8), contains the most luminous galaxy of the sample (NGC 1407), and yet does not lie at what could be termed the “central” parts of the cluster. In general, the luminosity distribution of the galaxies in the clumps does not show any other special characteristic. The crossing times are all less than 0.1

Hubble time, and are at least a factor of 5 smaller than the crossing time of the cluster as whole.

It is interesting to note that most of the early-type galaxies are concentrated in clumps A and B, where the population mix is 1/4/3 (13%/50%/37%) and 1/3/1 (20%/60%/20%), respectively. From Table III it can be seen that the total mass obtained by summing the individual masses of subclusters is slightly larger than that obtained in Table II for the cluster.

The existence of all these massive subcomponents, as well as the irregular appearance of the cluster, makes a realistic interpretation of the dynamical state of Eridanus very complicated, particularly as the assumption of virialization may not be fully satisfied. However, since all of the individual subclusters have small crossing times, we will assume as a first approximation that they are in a virialized regime.

To determine whether these clumps form a gravitationally bound system, we have used two methods. The first is by calculating the total energy of the association of clumps and comparing the kinetic to the potential energy (Materne 1974). Using the virial masses from Table IV we find that the total energy is negative and that the potential energy is larger than the kinetic by a factor of about 18; this is prob-

TABLE IV. Dynamical parameters of subclusters.

G	N	α	δ	cz +/- (km/s)	σ_v	R_H +/- (Mpc)	R_p +/-	M_{VT} +/- ($10^{13} M_\odot$)	M_p +/-	M_{pv} +/-	T_c
A	8	3 ^h 38.2 ^m	-18°46'	1739 45	409	0.48 0.02	0.25 0.01	5.5 0.3	8.8 4.6	3.2 0.3	0.03
B	5	3 ^h 37.4 ^m	-23°03'	1618 64	338	0.40 0.04	0.21 0.01	3.0 0.3	4.0 2.7	1.2 0.5	0.03
C	6	3 ^h 23.2 ^m	-21°32'	1554 57	285	0.26 0.05	0.17 0.01	1.4 0.3	0.9 0.4	1.0 0.2	0.02

ably larger than the uncertainties associated to the mass determination. This indicates that the substructures do form a bound system.

The other method is through testing the Newtonian binding conditions for linear orbits (Bothun *et al.* 1983; Beers Geller, and Huchra 1982, hereafter referred to as BGH):

$$V_r^2 R_p < 0.76 G \mathcal{M}_t,$$

where V_r is the relative radial velocity between any two clumps, R_p is their projected separation, and \mathcal{M}_t the total mass of the two clumps. The advantage of this method is that the gravitational binding of the two bodies is underestimated (BGH). Using the parameters from Table IV we find that by combining the clumps two by two, all subclusters are gravitationally bound, confirming the results obtained above. We did not use the full approach of BGH because, in this case, we have three clumps of similar masses that are fairly close to each other, so a two-body model of point masses is not adequate. Another problem is the uncertainty in the determination of the masses, which may be affected by interlopers, particularly in the case of clump A, where one galaxy has a radial velocity that is much smaller than the average for the clump. In addition, the small number of members can also lead to large errors in the velocity dispersion, and consequently in the calculation of the mass. These uncertainties prevent an assessment of whether coalescence of the clumps will actually take place and in what timescale.

As mentioned earlier, Eridanus lies in a filamentary structure together with Fornax, from which it is separated by about 3 Mpc (on the plane of the sky), suggesting that these systems may be bound. To answer that question we have used the two-body approach of BGH, as well as their basic assumptions, i.e., that both clusters can be considered as point masses, started from the same point at $t = 0$ moving in radial orbits, and that $q_0 = 0$. The orbital equations are then given by

$$R = R_m (1 - \cos \chi)/2,$$

$$t = (R_m^3 / 8G \mathcal{M}_t)^{1/2} (\chi - \sin \chi),$$

$$v = (2G \mathcal{M}_t / R_m)^{1/2} \sin \chi / (1 - \cos \chi)$$

for the bound case. R is the linear separation at a time t , R_m is the separation at maximum expansion, \mathcal{M}_t is again the total mass, χ is the developmental angle, and v is the relative velocity of the clusters. These are related to observable parameters through

$$R_p = R \cos \alpha,$$

$$V_r = v \sin \alpha,$$

where α is the angle between the radius vector connecting both particles and the plane of the sky. To solve these equations we have used the mass of Eridanus given in Table II and for Fornax the mass determined by MdCL (their group no. 52). This analysis indicates that these clusters are bound, but on an outgoing orbit, moving at a relative velocity of 340 km/s, and separated by a radial distance of 6.0 Mpc. Maximum expansion will be attained in 4.4×10^{10} yr, at a distance of 12.1 Mpc. At such large separations the two-body approximation may break down because of the interaction with other systems, so that any inference on the future evolution of this binary system would be quite uncertain.

V. CONCLUSION

In this paper, we have made a study of the Eridanus group using the data available in the SGC. It was shown that Eridanus is an irregular and complex system that is apparently made up of various clumps that are gravitationally bound. The clumpiness of this group has not been detected at a high significance level by some of the proposed statistical tests, but we must stress that these tests have been designed primarily to detect either inhomogeneities superimposed over a regular distribution, or the presence of a binary system, neither being the case of Eridanus. We have found that the clumps forming the Eridanus system have very different morphological populations, which may indicate that the morphological types of galaxies are set prior to the formation of rich clusters, as expected in the cold dark matter theories. The importance of studying a system like Eridanus is that its present dynamical stage may represent an important phase of cluster formation, and yet similar systems would go undetected at larger distances.

Eridanus lies in a filamentary structure that contains two other groups, Fornax and Dorado. In the present work we have shown that Eridanus and Fornax form a gravitationally bound system, as previously suggested by Welch, Chincarini, and Rood (1975), but which are presently separating, reaching maximum expansion in a few 10^{10} yr. The results of our analysis of Eridanus suggest that the formation of rich clusters ($\mathcal{M} > 10^{14} \mathcal{M}_\odot$) is likely to be still occurring at the present epoch, due to the merging of smaller groups.

We would like to thank M. Geller for her suggestions, M. A. G. Maia for discussions, and M. West for sending results in advance of publication. We also thank our collaborators in the SGC project for allowing us to use the data before publication. P. F. acknowledges a CNPq fellowship.

REFERENCES

- Bahcall, N. A. (1977). *Annu. Rev. Astron. Astrophys.* **15**, 505.
 Baier, F. W. (1983). *Astron. Nachr.* **304**, 211.
 Baker, R. H. (1933). *Ann. Harv. Coll. Obs.* **88**, 79.
 Baker, R. H. (1936). *Ann. Harv. Coll. Obs.* **88**, No. 6.
 Beers, T. C., Geller, M. J., and Huchra, J. P. (1982). *Astrophys. J.* **274**, 491 (BGH).
 Beers, T. C., Geller, M. J., Huchra, J. P., Latham, D. W., and Davis, R. J. (1984). *Astrophys. J.* **283**, 33.
 Binggeli, B., Tammann, G. A., and Sandage, A. (1987). *Astron. J.* **94**, 251.
 Bothun, G. D., Geller, M. J., Beers, T. C., and Huchra, J. P. (1983). *Astrophys. J.* **268**, 47.
 da Costa, L. N., Pellegrini, P. S., Sargent, W. L. W., Tonry, J., Davis, M. Meiksin, A., Latham, D. W., Menzies, J. W., and Coulson, I. A. (1988). *Astrophys. J.* **327**, 544.
 Danese, L., De Zotti, G., and di Tullio, G. (1980). *Astron. Astrophys.* **82**, 322.
 Dressler, A., and Shectman, S. A. (1988). *Astron. J.* **95**, 985.
 Fitchett, M. (1988). *Mon. Not. R. Astron. Soc.* **230**, 161.
 Fitchett, M., and Merritt, D. (1988). *Astrophys. J.* **335**, 18.
 Fitchett, M. and Webster, R. (1987). *Astrophys. J.* **317**, 653.
 Geller, M. J. (1988). In *17th Advanced Course of the Swiss Society of Astronomy and Astrophysics*, edited by L. Martinet and M. Mayor (Geneva Observatory, Sauverny), p. 69.
 Geller, M. J., and Beers, T. C. (1982). *Publ. Astron. Soc. Pac.* **94**, 421.
 Geller, M. J., Beers, T. C., Bothun, G. D., and Huchra, J. P. (1984). *Astron. J.* **89**, 319.

- Geller, M. J. and Huchra, J. P. (1983). *Astrophys. J. Suppl.* **52**, 61.
- Heisler, J., Tremaine, S., and Bahcall, J. N. (1985). *Astrophys. J.* **298**, 8.
- Hill, J. M., Hintzen, P., Oegerle, W. R., Romanishin, W., Lesser, M. P., Eisenhamer, J. D., and Batuski, D. J. (1988). *Astrophys. J. Lett.* **332**, L23.
- Hopp, U., and Materne, J. (1985). *Astron. Astrophys. Suppl.* **61**, 93.
- Huchra, J. (1976). *Astron. J.* **81**, 952.
- Huchra, J. P., and Geller, M. J. (1982). *Astrophys. J.* **257**, 423.
- Lauberts, A. (1982). *The ESO / Uppsala Catalogue of the ESO(B) Atlas* (European Southern Observatory, Garching).
- Maia, M. A. G., da Costa, L. N., and Latham, D. W. (1988). *Astrophys. J. Suppl.* **69**, 809 (MdCL).
- Materne, J. (1974). *Astron. Astrophys.* **33**, 451.
- Oegerle, W. R., Fitchett, M. J., and Hoessel, J. G. (1989). *Astron. J.* **97**, 627.
- Pearson, E. S., and Hartley, H. O. (1970). *Biometrika Tables for Statisticians* (Cambridge University, Cambridge).
- Pearson, E. S., and Stephens, M. A. (1964). *Biometrika* **51**, 484.
- Pellegrini, P. S. S. (1988). Ph.D. thesis, Publicação Especial No. 10, Observatório Nacional, Rio de Janeiro.
- Pellegrini, P. S., da Costa, L. N., Huchra, J. P., Latham, D. W., and Willmer, C. N. A. (1989). *Astron. J.* (submitted).
- Rood, H. J., Rothman, V. C. A., and Turnrose, B. E. (1970). *Astrophys. J.* **162**, 411.
- Sandage, A., and Tammann, G. A. (1975). *Astrophys. J.* **196**, 313.
- Sharples, R. M., Ellis, R. S., and Gray, P. M. (1988). *Mon. Not. R. Astron. Soc.* **231**, 479.
- de Vaucouleurs, G. (1975). In *Galaxies and the Universe*, edited by A. Sandage, M. Sandage, and J. Kristian (University of Chicago, Chicago), p. 557.
- Vorontsov-Velyaminov, B. A., and Arhipova, V. P. (1963–1968). *Morphological Catalogue of Galaxies*, Parts 2–4 (Moscow University, Moscow).
- Welch, G. A., Chincarini, G., and Rood, H. J. (1975). *Astron. J.* **80**, 77.
- West, M. J., and Bothun, G. D. (1988). Preprint (WB).
- West, M. J., Oemler, A., and Dekel, A. (1988). *Astrophys. J.* **327**, 1 (WOD).
- Yahil, A., and Vidal, N. V. (1977). *Astrophys. J.* **214**, 347.
- Zwicky, F., Herzog, E., Wild, P., Karpowicz, M., and Kowal, C. (1961–1968). *Catalogue of Galaxies and Cluster of Galaxies*, Vols. 1–6 (California Institute of Technology, Pasadena).